BJP BRITISH JOURNAL OF PHARMACOLOGY

BPS BRITISH PHARMACOLOGICAL SOCIETY

British Journal of Pharmacology (2010), 160, 283–291

0007-1188/10
www.brjpharmacol.org

RESEARCH PAPER

Atomoxetine acts as an NMDA receptor blocker in clinically relevant concentrations

Andrea G Ludolph[1,2], Patrick T Udvardi[1,2], Ulrike Schaz[2], Carolin Henes[1], Oliver Adolph[3], Henry U Weigt[3], Joerg M Fegert[1], Tobias M Boeckers[2] and Karl J Föhr[3]

[1]*Department of Child and Adolescent Psychiatry, University of Ulm, Ulm, Germany,* [2]*Institute of Anatomy and Cell Biology, University of Ulm, Ulm, Germany, and* [3]*Department of Anaesthesiology, University of Ulm, Ulm, Germany*

Background and purpose: There is increasing evidence that not only the monoaminergic but also the glutamatergic system is involved in the pathophysiology of attention-deficit hyperactivity disorder (ADHD). Hyperactivity of glutamate metabolism might be causally related to a hypoactive state in the dopaminergic system. Atomoxetine, a selective noradrenaline reuptake inhibitor, is the first non-stimulant approved for the treatment of this disorder. Here we have evaluated the effects of atomoxetine on glutamate receptors *in vitro*.
Experimental approach: The whole-cell configuration of the patch-clamp technique was used to analyse the effect of atomoxetine on *N*-methyl-D-aspartate (NMDA) receptors in cultured rodent cortical and hippocampal neurons as well as on NMDA receptors heterologously expressed in human TsA cells.
Key results: Atomoxetine blocked NMDA-induced membrane currents. Half-maximal inhibition emerged at about 3 μM which is in the range of clinically relevant concentrations found in plasma of patients treated with this drug. The inhibition was voltage-dependent, indicating an open-channel blocking mechanism. Furthermore, the inhibitory potency of atomoxetine did not vary when measured on NMDA receptors from different brain regions or with different subunit compositions.
Conclusions and implications: The effective NMDA receptor antagonism by atomoxetine at low micromolar concentrations may be relevant to its clinical effects in the treatment of ADHD. Our data provide further evidence that altered glutamatergic transmission might play a role in ADHD pathophysiology.
British Journal of Pharmacology (2010) **160,** 283–291; doi:10.1111/j.1476-5381.2010.00707.x

Keywords: ADHD; atomoxetine; transporter inhibitor; glutamate metabolism; NMDA receptor; whole cell patch clamp

Abbreviations: ADHD, attention-deficit hyperactivity disorder; CYP2D6, cytochrome P-450 2D6 enzyme; DAT, dopamine transporter; E18, embryonic day 18; GluN1, NMDA receptor subunit; GluN2A, NMDA receptor subunit; GluN2B, NMDA receptor subunit; K_i, inhibition constant; MEM, Minimum Essential Medium; NET, noradrenaline transporter; NMDA, *N*-methyl-D-aspartate; SHR, spontaneously hypertensive rat

Introduction

Attention-deficit hyperactivity disorder (ADHD) is the most frequently diagnosed neuropsychiatric disorder in childhood with an estimated prevalence of 5% worldwide (Polanczyk *et al.*, 2007). The three cardinal symptoms are hyperactivity, inattention and impulsivity (Biederman and Faraone, 2005). The psychostimulant methylphenidate, a substance of first choice in the treatment of ADHD with the remarkable effect size of about 1.0 in different patient groups (Szobot *et al.*, 2004; Findling *et al.*, 2007a), is an inhibitor of the presynaptic dopamine transporter (DAT). It is still under discussion whether alterations of the dopaminergic system are the primary pathophysiological cause for ADHD symptoms or the sequelae of other underlying neurobiological mechanisms such as hyperactivity in the glutamatergic system (Carrey *et al.*, 2007; Lulé *et al.*, 2008). Moreover, it is still unclear if other deficiencies, for instance, in the noradrenergic, serotonergic or GABAergic systems, play a role. In spite of the high effect sizes in acute treatment, the long-term outcome in ADHD is not satisfying, not even after methylphenidate treatment for years. In the 8 year follow-up of the Multimodal Treatment study of children with ADHD (n = 487), some children showed substantial long-term benefit from medication while others showed little improvement (Molina *et al.*, 2009). Therefore, alternative treatment options are in great demand. As the first non-stimulant medication, atomoxetine

Correspondence: Andrea G Ludolph, Department of Child and Adolescent Psychiatry, University of Ulm, Steinhoevelstrasse 5, 89075 Ulm, Germany. E-mail: andrea.ludolph@uni-ulm.de
Received 23 July 2009; revised 19 October 2009; accepted 8 November 2009

was approved for ADHD treatment in 2002. Atomoxetine is supposed to bind selectively to the presynaptic noradrenaline transporter (NET) (enzyme inhibition constant [K_i] ~ 4.5 nmol·L^{-1}), with minimal affinity for the other monoamine transporters or receptors (Swanson *et al*., 2006; Michelson *et al*., 2007). Methylphenidate and atomoxetine increase both noradrenaline and dopamine in prefrontal cortex and show similar inhibitory and excitatory effects on motor cortex (Gilbert *et al*., 2006). But whereas methylphenidate is effective within 30–60 min, the therapeutic effect of atomoxetine takes at least 2–3 up to 6 weeks to develop. This fact questions the assumption that the effect is solely mediated by the rapid blockade of the NET which could be detected in experimental studies (Seneca *et al*., 2006).

Atomoxetine's chemical structure resembles that of fluoxetine, the most commonly used selective 5-HT reuptake inhibitor. The only difference is a methyl group in the *ortho* position instead of the trifluoromethyl group in the *para* position. Hence, it seems to be reasonable to investigate if some of fluoxetine's properties are also relevant for atomoxetine. In a recent study, a direct inhibiting effect of fluoxetine on *N*-methyl-D-aspartate (NMDA) receptors could be demonstrated (Szasz *et al*., 2007). Therefore, we investigated the possible impact of atomoxetine on NMDA receptors by means of the patch clamp technique in rodent embryonic cortical and hippocampal neurons.

Methods

Cell culture

Different types of NMDA receptor-containing cells were used, i.e. primary neurons cultured from the cortex and the hippocampus of the rat and TsA201 cells transfected with cDNAs encoding for NMDA receptors.

Primary cultures of embryonic cortical and hippocampal neurons from the rat were prepared according to Goslin and Banker (1989) modified by Dresbach *et al*. (2003). In brief, cortices and hippocampi from E18 rat embryos were digested using trypsin (0.25%) and DNase 1 (48 U) for 15 min at 37°C. Thereafter, the tissue was mechanically dissociated in Dulbecco's modified Eagle medium supplemented with 10% fetal calf serum, 2% B27, 50 U·mL^{-1} penicillin, 50 µg·mL^{-1} streptomycin and 2 mM glutamine. The cells were then plated at a density of 1.5×10^5 cells per glass coverslip, pre-coated with poly-L-lysine (50 µg·mL^{-1}). After 24 h the medium was exchanged for neurobasal medium containing 50 U·mL^{-1} penicillin, 50 µg·mL^{-1} streptomycin, 2 mM glutamine, and 1% B27 and cultured at 37°C in a humidified atmosphere with 5% CO_2.

The TsA201 cell line is a derivative of the human embryonic kidney cell line HEK-293 (ATCC#CRL1537), which expresses a T-antigen against the simian virus 40. TsA cells were cultured at 37°C in a humidified atmosphere at 95% air and 5% CO_2 in MEM supplemented with 50 U·mL^{-1} penicillin, 50 µg·mL^{-1} streptomycin (Gibco, Eggenstein, Germany), 2 mM L-glutamine (Boehringer, Mannheim, Germany), and 10% fetal calf serum (Gibco). The cells were grown on polyornithine-coated culture dishes to 40% confluency and transfected using the Trans-Fektion™ kit (Bio-Rad, München, Germany). For the construction of NMDA receptors (nomenclature follows Alexander *et al*., 2008), the subunits GluN1 (Moriyoshi *et al*., 1991) and GluN2A or GluN2B (Kutsuwada *et al*., 1992; Monyer *et al*., 1994) were used. After transfection, ketamine (200 µM) was added to the culture medium.

Electrophysiology

Electrophysiological experiments were performed with neurons cultivated for 8–14 days or with TsA cells 24–48 h after transfection. Membrane currents were recorded in the whole-cell recording mode using an EPC-9 amplifier and TIDA software (HEKA, Lambrecht, Germany) (Hamill *et al*., 1981). Before recording, the cells were rinsed twice with extracellular standard solution composed of (in mM): 140 NaCl, 2.7 KCl, 1.5 $CaCl_2$, 10 glucose and 12 HEPES; pH 7.3, supplemented with strychnine (100 µM) and tetrodotoxin (TTX; 50 nM). This solution was also used for the analysis of transfected TsA cells, if not stated otherwise. Patch pipettes were drawn from borosilicate glass with tip resistances between 3 and 6 MΩ when filled with (in mM) 140 $CsCl_2$, 2 $MgCl_2$, 2 ATPx2Na, 2 EGTA, 10 HEPES; pH 7.2. In order to minimize Ca^{2+}-dependent receptor inactivation and/or desensitization and to avoid possible effects of the ion channel blockers (see above), we reduced the Ca^{2+} concentration to 0.3 mM and added no ion channel blockers. This extracellular low Ca^{2+} solution was solely employed for the analysis of heterologously expressed NMDA receptors when indicated. In these experiments EGTA in the internal solution was replaced by BAPTA (2 mM). To improve sealing, tips were briefly dipped into 2% dimethylsilane dissolved in dichlormethane. Unless otherwise stated all experiments were performed at room temperature and the membrane potential clamped to –80 mV.

Drug application

The medium in the dish (1.5 mL) was continuously exchanged using a 'global' bath perfusion with the inflow set at 4.5 mL·min^{-1} and the outflow removing any excess fluid. Reagents were applied to the cells using the L/M-SPS-8 superfusion system (List, Darmstadt, Germany). To restrict the presence of the reagent to a small volume within the dish a 'local' bath perfusion was used that generated a continuous flow of the reagent in the desired concentration. The local inlet (tip of an eight-barrelled pipette) was positioned at a distance of 50–100 µm upstream and the local outlet at about 300 µm downstream of the measuring field. The selection among the eight vessels connected to the eight-barrelled pipette was controlled with magnetic valves. A constant flow rate of control and test solutions (1 mL·min^{-1}) was achieved by means of a pressure control system (MPCU-3, Lorenz, Göttingen, Germany). The time of solution exchange was estimated from the changes in the liquid junction potential to be about 1 ms. Using this system, current rise times (10–90%) of around 6 ms were achieved by application of 3 mM glutamate to cultivated neurons (Dinse *et al*., 2005).

Data analysis

Concentration–inhibition curves were fit to the Hill Equation (1):

$$I_{rel} = I_{control} / \left[1 + ([B]/IC_{50})^{n}\right] \quad (1)$$

Where $I_{control}$ is the current amplitude in the absence and I_{rel} in the presence of the blocker. [B] is the concentration of the blocker, IC_{50} is the concentration of the blocker that causes 50% inhibition and n is the Hill coefficient.

For the analysis of the voltage-dependence of block by atomoxetine, data were analysed using the model of Woodhull (1973) by fitting the data to Equation (2):

$$I_{rel} = K_{(0)} / \{(K_{(0)} + [B] * \exp(-z\delta FV/RT)\} \quad (2)$$

I_{rel} is the relative amplitude of the current in the presence of the blocker. $K_{(0)}$ is the equilibrium dissociation constant at 0 mV. [B] is the concentration of the blocker, *z* is the valence of the blocker, δ is the electric distance across the electric field of the membrane at which the blocker becomes bound; *V*, *F*, *R* and *T* are the membrane voltage, Faraday's constant, gas constant and the absolute temperature respectively. Curve fitting was performed using SigmaPlot 10.0 software (Sysstat, San Jose, CA, USA).

On- and off-rate constants were estimated from τ_{on} and τ_{off} according to the Equations (3,4):

$$k_{off} = 1/\tau_{off} \quad (3)$$

$$k_{on} = (1/\tau_{on} - 1/\tau_{off})/[A] \quad (4)$$

τ_{on} and τ_{off} are the time constants obtained from on- and offset of inhibition upon the application and removal of atomoxetine in the continuous presence of agonists. k_{on} and k_{off} are the rate constants calculated according to formula 3,4. [A] represents the concentration of atomoxetine.

Statistical analysis

Statistical significance was determined using ANOVA to compare many groups or using the unpaired *t*-test when comparing the mean results from two groups. A difference between results was considered significant when $P < 0.05$. Results are presented as means ± SD.

Materials

Dulbecco's modified Eagle medium, Hank's balanced salt solution, Neurobasal, B27, penicillin/streptomycin, glutamine were from Gibco BRL (Eggenstein, Germany); trypsin was from Biochrom AG (Berlin, Germany); DNase 1 from Invitrogen (Carlsbad, Germany); fetal calf serum from HyClone, Perbio Science (Bonn, Germany) and poly-L-lysine from Sigma-Aldrich (Schnelldorf, Germany). Atomoxetine and all other chemicals were from Sigma-Aldrich Chemie GmbH (Steinheim, Germany).

Results

Reversible inhibition of NMDA-evoked membrane currents of cortical neurons by atomoxetine

Application of 100 µM NMDA in the presence of 10 µM glycine in extracellular standard solution to rat cortical neurons induced a fast inward current (peak) which declined to a stable steady-state current (plateau) at the end of a 20 s drug application. In the presence of 25 µM atomoxetine, predominantly the plateau currents were reduced, whereas peak currents were almost unaffected. As a control application after a 60 s washout period revealed that recovery from inhibition was still incomplete, an additional control current was evoked (Figure 1A). In order to establish a concentration–inhibition relationship we tested atomoxetine in a range from 0.75 to 50 µM in the presence of 100 µM NMDA. For the evaluation we compared the amplitudes of the plateau currents in the presence (I_{rel}) and absence ($I_{control}$) of atomoxetine. To consider the commonly observed phenomenon of current run-down during repeated and prolonged applications of high concentrations of NMDA which amounted to 19.2 ± 5.3% (*n* = 6–8)

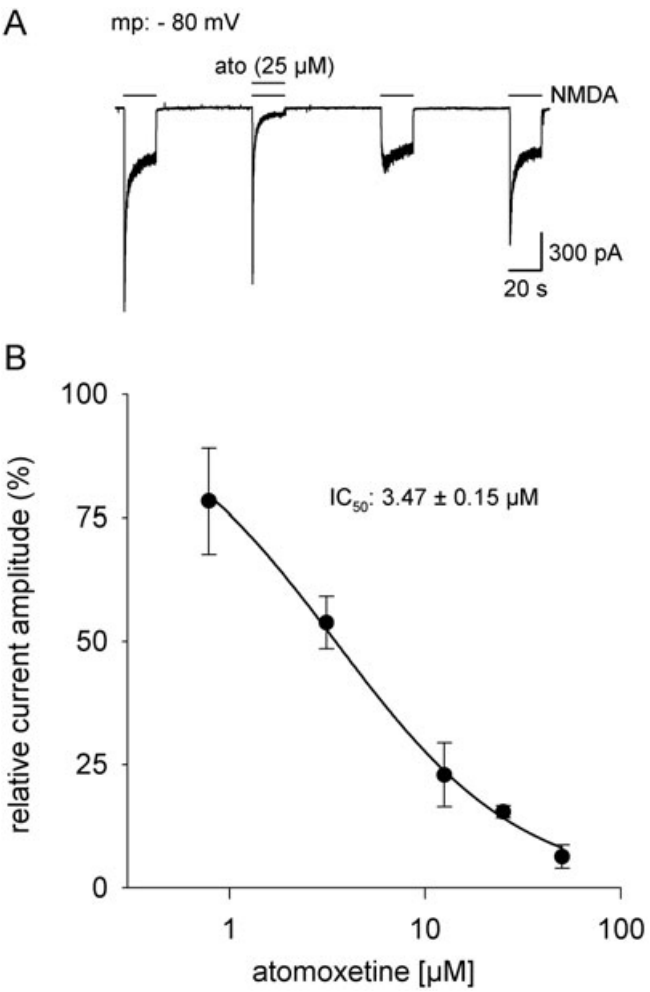

Figure 1 Inhibition of NMDA-induced membrane currents in cortical neurons by atomoxetine. (A) Experimental protocol showing a typical current trace recorded from cortical neurons. Agonists (100 µM NMDA + 10 µM glycine) were repeatedly applied for 20 s intermitted by washout periods of 60 s. Membrane potential was held at –80 mV. Co-application of atomoxetine reversibly reduced the steady-state current measured at the end of drug application. (B) Concentration–inhibition relationship for different concentrations of atomoxetine. Experiments were performed as shown in A. Data points represent the relative current amplitude in percentage to control, resulting in an IC_{50} of 3.47 ± 0.15 µM. Data from 4 to 6 cells are shown as the mean ± SD.

between first and last control and the mentioned delayed recovery from inhibition, we used the mean of the first and the last application as control ($I_{control}$). The resulting data for I_{rel} were plotted against the concentration of atomoxetine and fitted with the Hill Equation (1). From the fit an IC_{50} of 3.47 ± 0.15 μM and a Hill coefficient of 0.9 were calculated (n = 5–6 cells) (Figure 1B).

From preliminary experiments we knew that the half-maximal effective NMDA concentration for plateau currents was 18.6 ± 1.2 μM and that the effect of atomoxetine on NMDA-induced currents was independent of the NMDA concentration in the range from 10 to 1000 μM, indicating a non-competitive interaction of atomoxetine with the NMDA receptor (n = 5 cells). To achieve reliable signal amplitudes we therefore used NMDA in a concentration of 100 μM which is near the maximal effective concentration, resulting in current amplitudes of 858 ± 440 pA (n = 38). Furthermore, long-lasting drug application times (20 s) were required, as the development of steady-state currents in the presence of atomoxetine was time and concentration-dependent, such that steady-state currents developed much slower at low concentrations of atomoxetine.

The inhibitory potency of atomoxetine is independent from the brain region and NMDA receptor subunit composition

In order to analyse whether atomoxetine differently affects NMDA receptors on neurons from different brain regions we measured the inhibitory potency of 3 and 25 μM atomoxetine at hippocampal and cortical neurons in extracellular standard solution. The inhibition was not significantly different for the two brain regions at either concentration of atomoxetine (Figure 2). As these neurons mainly express the GluN2B subunit at this developmental stage (Szasz *et al*., 2007), we extended our experiments to a heterologous expression system in order to detect a possible difference in the sensitivity for GluN2A and GluN2B receptors. No difference in the inhibitory potency of atomoxetine between GluN2A and GluN2B containing receptors was found (Figure 2).

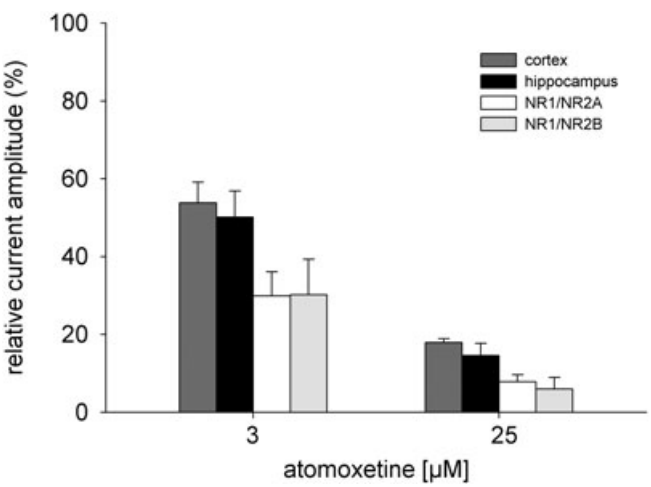

Figure 2 Inhibitory potency of atomoxetine at native and heterologously expressed NMDA receptors. NMDA/glycine-induced membrane currents in the presence of 3 or 25 μM atomoxetine are shown as % control values. The inhibitory potency of atomoxetine at cortical and hippocampal neurons as well as at GluN1/GluN2A and GluN1/GluN2B receptors expressed in TsA cells is illustrated. Experiments were performed as described in Figure 1A. Data obtained from 4 to 6 individual cells are presented as mean ± SD. There was no statistically significant difference between the different groups (P > 0.05).

To suppress spontaneous neuronal activity, strychnine and TTX were present in the standard extracellular solution. As strychnine is known to operate as a weak open-channel blocker, we additionally tested the effect of atomoxetine on the GluN2A subunit without these blockers (Bertolino and Vicini, 1988). Expectedly, the inhibition was stronger in the absence of the blockers. The IC_{50} values calculated according to the Hill equation were 3.2 ± 0.18 μM in the presence and 1.58 ± 0.13 μM in the absence of the blockers (n = 4–5 cells).

Mechanism of inhibition of NMDA-evoked currents by atomoxetine

Our results showed a non-competitive NMDA receptor antagonism of atomoxetine. Therefore, we tested whether the mechanism of inhibition was that of an open-channel blocker. Common criteria for open-channel blockers are that the degree of inhibition occurs in a voltage- and use-dependent manner. In a first set of experiments we performed electrophysiological recordings with the extracellular standard solution at different membrane potentials ranging from –80 mV to +40 mV while the concentration of the agonists (100 μM NMDA/10 μM glycine) and that of the antagonist (25 μM atomoxetine) were kept constant (Figure 3). As shown in Figure 3B, the inhibitory effect was clearly voltage-dependent, so that the inhibition was attenuated by depolarization (compare original traces of Figures 1A and 3A). Additional experiments, conducted in order to differentiate between a true voltage-dependent channel block and a modulation by Ca^{2+}-dependent inactivation/desensitization processes, also showed voltage dependence. For this purpose we tested heterologously expressed GluN1/GluN2A receptors using the extracellular low Ca^{2+} solution and a low agonist concentration (10 μM NMDA). Under these conditions receptor desensitization was marginal or even absent and the current run-down between the first and last NMDA application was 6.3 ± 2.9% (n = 4). However, the voltage dependence of block by atomoxetine was the same under standard and low extracellular Ca^{2+} solution.

According to the Woodhull model (Equation 2), we calculated for our external standard solution a δ-value of 0.74 for the location of the binding site of atomoxetine within the electric field of the membrane and a theoretical IC_{50} of 32.4 ± 1.1 μM (n = 4–6 cells) at 0 mV. The corresponding values obtained with the extracellular low Ca^{2+} solution were 0.83 and 33.4 ± 1.9 μM (n = 4–6 cells).

To look for a possible use-dependent blocking mechanism we used two different experimental designs. In a first set-up we analysed current amplitudes obtained from repeated short-term (2 s) applications of agonists (10 μM NMDA + 10 μM glycine) in the absence or continuous presence of atomoxetine (25 μM) (Figure 4, left). Using the extracellular low Ca^{2+} solution, control currents revealed a run-down of 4.7 ± 1.7% from the first to the last (12th) agonist application. When atomoxetine was superfused, inhibition of evoked

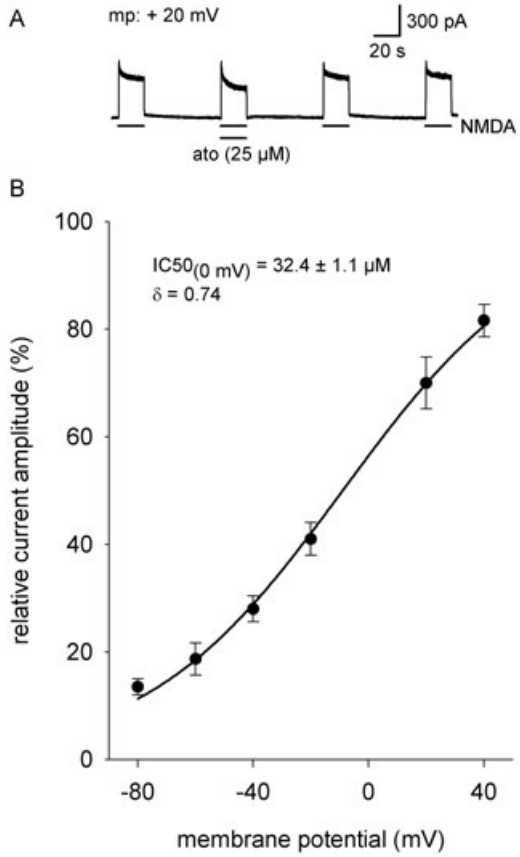

Figure 3 Voltage-dependent block of NMDA-induced membrane currents in cortical neurons by atomoxetine. (A) Agonists (100 µM NMDA + 10 µM glycine) were repeatedly applied to cortical neurons for 20 s intermitted by washout periods of 60 s while the membrane potential was held at +20 mV. Co-application of atomoxetine (25 µM) shows a reduced inhibitory potency compared with the membrane potential at −80 mV (see Figure 1A). (B) Summary of experiments showing the relative current amplitudes in the presence of 25 µM atomoxetine at different membrane potentials. The degree of plateau current inhibition diminishes with membrane depolarization. Fitting the data according to Equation 2 (Woodhull model) revealed a δ-value of 0.74. Data from 4 to 6 cells are presented as mean ± SD.

currents continuously increased from 36.6 ± 12.6% to 91.4 ± 2.8%. During washout (six control applications), current amplitudes recovered to 58.7 ± 2.4% of first control (n = 3 cells; data not corrected for run-down).

In order to differentiate whether this time-dependent increase in inhibition required the activation of the channel we compared the time course of inhibition obtained from long-term (20 s) applications of co-application of agonists and atomoxetine, with that obtained after a pre-incubation of atomoxetine for 20 s (Figure 4, right). The time course of inhibition was identical under both conditions. In detail, time constants without (2.04 ± 0.32 s) and after pre-incubation of atomoxetine (1.93 ± 0.31 s) were not significantly different (n = 6–8 cells; $P > 0.05$). These results provide further evidence that atomoxetine blocks NMDA receptors in an use-dependent manner. So, atomoxetine fulfils yet another criterion to be an open-channel blocker of NMDA receptors.

Evidence for interference between the Mg^{2+} and the atomoxetine-binding site

As our calculations indicated a binding site deep within the channel pore, it was reasonable to assume that atomoxetine might interact with the binding site for Mg^{2+} ions. In order to test this hypothesis we compared offset time constants at GluN1/GluN2A receptors because of the application of Mg^{2+} ions (5 mM) or atomoxetine (25 µM) alone, with that of their combined application (Figure 5). Note, that Mg^{2+} ions had been pre-incubated for 10 s before the combination was tested. Using the extracellular low Ca solution, offset time constants (τ_{off}) were estimated to be 115 ± 36 ms for Mg^{2+} ions, 21 960 ± 6062 ms for atomoxetine and 124 ± 34 ms for Mg^{2+} plus atomoxetine (n = 4 cells). As the offset time constants for Mg^{2+} alone and Mg^{2+} plus atomoxetine are nearly identical, it can be assumed that Mg^{2+} ions had prevented atomoxetine from interacting with its binding site. Thus, these data suggest that Mg^{2+} and atomoxetine are likely to have a common interaction site at the NMDA receptor.

These measurements are also the basis for the calculation of k_{on} and k_{off} rate constants for atomoxetine. According to Equations (3,4), k_{on} was calculated to be 1.86×10^4 M^{-1} s^{-1} and k_{off} was calculated to be 0.048 s^{-1} (n = 4–5 cells).

Discussion

The main finding of our investigation is that atomoxetine blocks NMDA receptors in low micromolar concentrations that are equivalent or even lower than those found in plasma of treated patients.

Mechanism of block

Our finding that atomoxetine interacts with NMDA receptors in a non-competitive manner indicates that atomoxetine might bind to the receptor apart from the ligand-binding site. In the case of ion channels, the term 'non-competitive' also includes sites located within the channel pore. Indeed, an open-channel blocking mechanism for atomoxetine is suggested from the voltage and use dependency of the block and the localization of the interaction site deep within the channel pore. The calculated δ-value for the electrical distance of 0.74 closely coincides with that for Mg^{2+} ions (0.78) (Sobolevsky and Yelshansky, 2000). Thus, it can be assumed that atomoxetine might interact with the Mg^{2+}-blocking site of the NR1 subunit of the NMDA receptor. This assumption is further strengthened by comparing offset time constants obtained from the application of Mg^{2+} ions, atomoxetine by themselves or a combination thereof. As the offset time constants for the co-application were identical with that of Mg^{2+} ions, it can be assumed that pre-application of Mg^{2+} ions had masked the binding site for atomoxetine. A similar behaviour has previously been observed with desipramine but not with fluoxetine (Szasz *et al.*, 2007). Whether other parts of the ion channel contribute to the interaction of atomoxetine within the channel pore, as reported for memantine remains to be shown (Chen and Lipton, 2005). Very recently, atomoxetine was shown to inhibit human Ether-à-Go-Go-Related Gene channels. Also here, an open-channel blocking mechanism

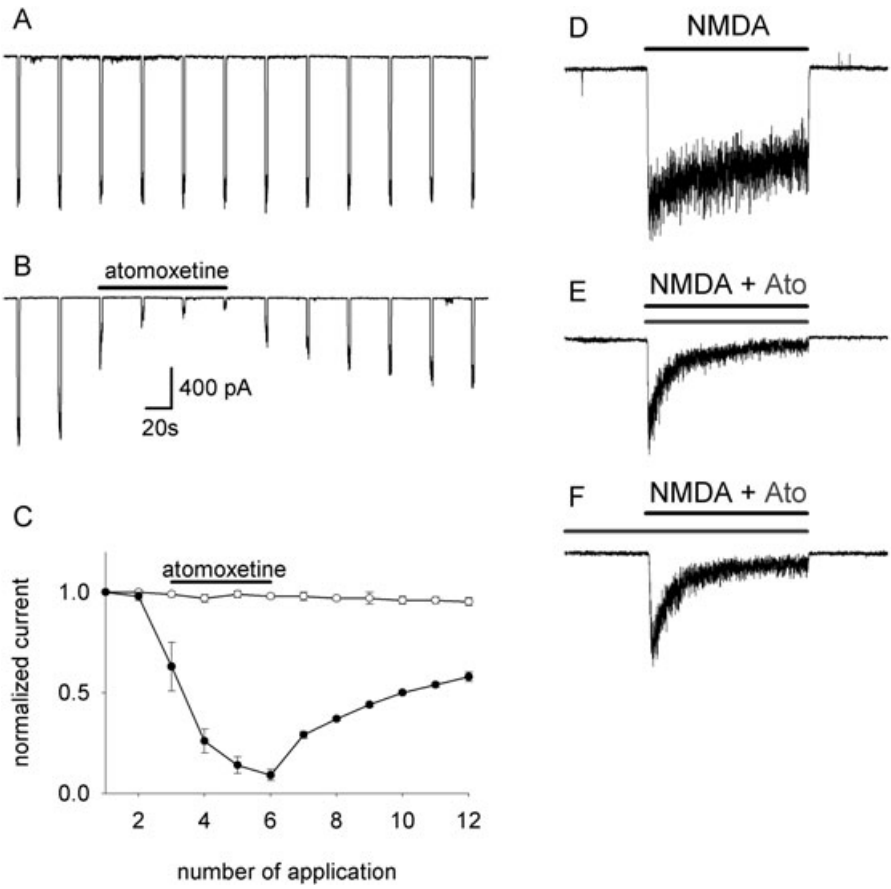

Figure 4 Use-dependent block of heterologously expressed NMDA receptors by atomoxetine. Typical current traces obtained from TsA cells, transfected with GluN1/GluN2A receptors after application of agonists (10 μM NMDA + 10 μM glycine) in the absence and presence of atomoxetine (25 μM). Left, repeated applications of agonists for 2 s every 30 s. (A) Control currents and (B) currents obtained in the continuous presence of atomoxetine as indicated by solid line. (C) Summary of current amplitudes, normalized to the first control current (n = 3 cells). Control currents are represented by open circles, currents in the presence of atomoxetine by closed circles. Right, typical current traces obtained from (D) application of agonists separately, (E) co-application of agonists and atomoxetine (Ato) and (F) pre-application of atomoxetine for 20 s before co-application. Time courses of current reduction by atomoxetine are identical in (E) and (F) (n = 4 cells). All experiments were performed in extracellular low Ca^{2+} solution with the membrane potential held at −80 mV.

was suggested, as the effect of atomoxetine was attenuated when pore mutants of this channel were analysed (Scherer *et al*., 2009).

Our finding that the inhibitory potency of atomoxetine was the same using neurons from different brain regions or heterologously expressed NMDA receptors containing GluN2A or GluN2B might also be related to its mechanism of action. Provided that atomoxetine exclusively interacts with the Mg^{2+}-binding site, we would expect that atomoxetine affects GluN2A or GluN2B subunit-containing receptors equally, as these receptors are almost identical in their sensitivity for Mg^{2+} ions (Wrighton *et al*., 2008). Furthermore, the lack of a difference in the responsiveness of cultivated hippocampal and cortical neurons is in line with these statements as these neurons primarily express the GluN2B subunit at this developmental stage (Szasz *et al*., 2007).

Antidepressants have previously been shown to modulate glutamatergic neurotransmission, a mechanism that presumably contributes to the antidepressant effect (reviewed in Pittenger and Duman, 2008). Atomoxetine is structurally very similar to fluoxetine. However, from its mechanism of action atomoxetine resembles desipramine which also operates as an open-channel blocker, whereas the binding site for fluoxetine seems to be outside the channel pore (Sernagor *et al*., 1989; Szasz *et al*., 2007). So far, no proved explanation can be offered for the different mechanisms of action of atomoxetine and fluoxetine. The hydrated trifluoromethyl group in the *para* position of fluoxetine instead of atomoxetine's simple methyl group in the *ortho* position, potentially leads to a different steric interaction which might prevent fluoxetine from entering the pore.

The IC_{50} at cortical neurons (about 3 μM) is well in the range of clinically relevant concentrations. *In vivo*, this value might even be lower as our experiments were conducted in the presence of strychnine which also interacts with the NMDA receptor by an open-channel blocking mechanism (Bertolino and Vicini, 1988). Our data, obtained with heterologously expressed NMDA receptors, revealed that in the absence of strychnine, the IC_{50} was reduced twofold. Thus, a similar reduction in the IC_{50} could be expected for cortical neurons under these conditions. Therefore, atomoxetine would be even more potent *in vivo*.

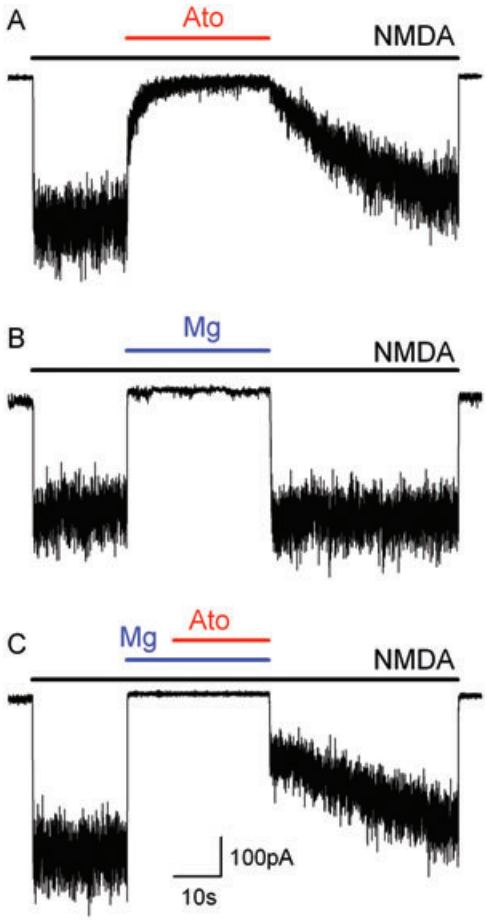

Figure 5 Inhibition of NMDA-induced membrane currents in the absence and presence of Mg^{2+} ions. Typical current traces obtained from TsA cells, transfected with GluN1/GluN2A receptors after (A) application of atomoxetine (Ato) (25 μM), (B) Mg^{2+} ions (5 mM) or (C) Mg^{2+} ions plus atomoxetine in the continuous presence of agonists (10 μM NMDA + 10 μM glycine). The time constants of τ_{off} upon removal of antagonists were 21 960 ± 6062 ms for atomoxetine, 115 ± 36 ms for Mg^{2+} and 124 ± 34 ms for Mg^{2+} plus atomoxetine (n = 4 cells). Note, the time constant in (C) represents the initial time constant immediately after removal of Mg^{2+} and atomoxetine. Measurements were performed in extracellular low Ca^{2+} solution with the membrane potential held at −80 mV.

Clinical implications

The core symptoms of ADHD can be effectively treated by psychostimulants for decades and recently also by atomoxetine, a NET inhibitor. As the main and best investigated effects of these substances are the inhibition of the presynaptic monoaminergic transporters, ADHD research primarily concentrated on the monoaminergic system. Assuming that the level of dopamine and noradrenaline might be too low in the synaptic cleft, the effect of psychostimulants and atomoxetine were mainly attributed to the inhibition of the presynaptic transporter molecules because the blocking of DAT and NET leads to an increased level of the neurotransmitters at the postsynaptic receptors. In the last years, preclinical and clinical data emerged that also alterations in other neurotransmitter systems, especially interactions with glutamate metabolism, might play a role in the pathophysiology of this highly prevalent and impairing disorder (Carrey *et al*., 2007; Lulé *et al*., 2008).

Lou (1996) was one of the first authors who considered that glutamate metabolism might also play a key role in the pathophysiology of ADHD. He pointed out that the striatum as an anatomical core structure in ADHD is highly vulnerable to ischaemia-induced liberation of glutamate, as glutamatergic afferent synaptic transmission from almost the entire cortex converge in the striatum. This fact might also explain the correlation between prematurity and high incidence of ADHD because prematurity often accompanies hypoxic–ischaemic events.

Jensen *et al*. (2009) hypothesized that abnormalities in the excitatory glutamatergic synaptic transmission might contribute to the altered behaviour in the spontaneously hypertensive rat (SHR) which is the best validated animal model of ADHD. They found a reduced synaptic transmission in hippocampal neurons of adult SHR compared with age-matched controls. Even more interestingly they described a similar long-term potentiation (LTP) in both groups but only in the SHR a significant LTP reduction by a GluN2B-specific receptor blocker. The blocker had no effect in the control group. As GluN2B receptors usually are functionally predominant at an early developmental stage (also in humans), this finding might point to an altered development of the glutamatergic system. In support of this, a genetic study in 205 families suggested an association between variations in the GluN2B subunit gene and ADHD (Dorval *et al*., 2007).

Do we have clinical evidence for a role of glutamatergic transmission in ADHD?

A proton magnetic resonance spectroscopy study investigated the glutamatergic system in the anterior cingulate cortex of children and adolescents with ADHD and with ADHD plus bipolar disorder, in comparison with controls (Moore *et al*., 2006). The authors revealed a significantly higher ratio of glutamate plus glutamine to myo-inositol-containing compounds in the ADHD children than in the healthy children.

Carrey *et al*. (2002) conducted a magnetic resonance spectroscopy study in four children, two of them had previously been treated with methylphenidate and the other two had been treated with atomoxetine. All four positively responded to treatment, only the two with atomoxetine showed changes in the glutamate/creatine ratio. Memantine, an uncompetitive NMDA receptor antagonist used for the treatment of Alzheimer's disease, was evaluated in an open-label pilot study for its effectiveness in paediatric patients with ADHD (Findling *et al*., 2007b). Two different doses, 10 mg·day^{-1} and 20 mg·day^{-1} were used. The higher dose was associated with a higher rate of completion and larger mean improvement on the clinical assessment scales.

Thus, a modulation of NMDA receptor activity might be at least part of an effective treatment for ADHD. We draw the conclusion from our data that the antagonism at NMDA receptors by atomoxetine might contribute to the clinical effect of this compound.

The effective concentrations used in this *in vitro* study are equivalent to plasma concentrations in treated patients. Atomoxetine is metabolized through the cytochrome P-450 2D6 (CYP2D6) enzyme pathway, which is genetically polymorphic in humans. These genetic variations lead to a bimodal

distribution of the pharmacokinetics with two distinct populations: extensive metabolizers and poor metabolizers (7% of Caucasians). In a study that evaluated the pharmacokinetics of atomoxetine in paediatric patients the atomoxetine C_{max} ($ng \cdot mL^{-1}$) observed ranged from 80 to 212 $ng \cdot mL^{-1}$ after a 10 mg single dose (Witcher *et al*., 2003). After a 20–45 mg twice daily regimens, the atomoxetine C_{max} observed ranged from 174 to 1221 $ng \cdot mL^{-1}$, the latter concentration close to 5 μM. All participants were extensive metabolizers. Studies performed as part of the atomoxetine clinical development programme suggest that total plasma exposure in poor metabolizers is approximately 10-fold higher when compared with extensive metabolizers (Sauer *et al*., 2005).

A very recent microdialysis evaluation in rats revealed a high brain penetration and an atomoxetine concentration in brain cells that is many times higher than in plasma (Kielbasa *et al*., 2009). However, it should be kept in mind that these concentrations do not necessarily represent the concentration in the biophase (Kielbasa *et al*., 2009). Plasma concentrations of atomoxetine are about several μM. To our knowledge, concentrations in the human brain have not yet been investigated. As the inhibition of the NMDA receptors took place in the low μM range in our *in vitro* study, this effect might well be relevant also *in vivo*.

In conclusion, we have found that atomoxetine exerted a dose-dependent antagonistic effect on NMDA receptors. The concentrations exerting 50% inhibition (IC_{50}) were comparable to, or even lower than the plasma concentrations measured under treatment (5 μM). Data are not available yet showing the atomoxetine concentrations achieved in the brain after clinical doses. Future clinical (imaging) and preclinical (*in vitro* and animal) studies will certainly help to assess the role of these novel mechanisms in neuropsychiatric disorders and their treatment.

Acknowledgements

We would like to thank Holger Lerche for helpful discussions and Eva Georgieff for help with data acquisition.

Conflict of interest

Dr Ludolph reports having received lecture fees from UCB/Celltech, Medice and Janssen, and research funding from UCB/Celltech and Medice. She is involved in clinical trials with Böhringer Ingelheim. Prof Fegert disclosed consulting fees and/or travel grants from Aventis, Bayer, Bristol-MS, J&J, Celltech/USB, Lilly, Medice, Novartis, Pfizer, Ratiopharm and Sanofi-Synthelabo. He was involved in clinical trials with Janssen, Medice, Lilly and Astra Zeneca, and has had unrestricted research grants from State and national governmental organizations and from the Volkswagen Foundation, the Eberhardt Foundation, from Eli Lilly Foundation, from Janssen and from UCB/Celltech. Patrick Udvardi, Dr Ulrike Schaz, Carolin Henes, Dr Adolph, Dr Weigt, Dr Boeckers and Dr Föhr reported no biomedical, financial interests or potential conflicts of interest.

References

Alexander SPH, Mathie A, Peters JA (2008). Guide to Receptors and Channels (GRAC), 3rd edition. *Br J Pharmacol* **153** (Suppl. 2): S1–S209.

Bertolino M, Vicini S (1988). Voltage-dependent block by strychnine of N-Methyl-D-Aspartic-acid-activated cationic channels in rat cortical neurons in culture. *Mol Pharmacol* **34**: 98–103.

Biederman J, Faraone SV (2005). Attention-deficit hyperactivity disorder. *Lancet* **366**: 237–248.

Carrey N, MacMaster FP, Sparkes SJ, Khan SC, Kusumakar V (2002). Glutamatergic changes with treatment in attention deficit hyperactivity disorder: a preliminary case series. *J Child Adolesc Psychopharmacol* **12**: 331–336.

Carrey NJ, MacMaster FP, Gaudet L, Schmidt MH (2007). Striatal creatine and glutamate/glutamine in attention-deficit/hyperactivity disorder. *J Child Adolesc Psychopharmacol* **17**: 11–17.

Chen HS, Lipton SA (2005). Pharmacological implications of two distinct mechanisms of interaction of memantine with N-Methyl-D-aspartate-gated channels. *J Pharmacol Exp Ther* **314**: 961–971.

Dinse A, Föhr KJ, Georgieff M, Beyer C, Bulling A, Weigt HU (2005). Xenon inhibits AMPA- and kainate-induced membrane currents in cortical neurons. *Brit J Anaesth* **94**: 479–485.

Dorval KM, Wigg KG, Crosbie J, Tannock R, Kennedy JL, Ickowicz A *et al*. (2007). Association of the glutamate receptor subunit gene GRIN2B with attention-deficit/hyperactivity disorder. *Genes Brain Behav* **6**: 444–452.

Dresbach T, Hempelmann A, Spilker C, tom Dieck S, Altroch WD, Zuschratter W *et al*. (2003). Functional regions of the presynaptic cytomatrix protein bassoon: significance for synaptic targeting and cytomatrix anchoring. *Mol Cell Neurosci* **23**: 279–291.

Findling RL, Short EJ, McNamara NK, Demeter CA, Stansbrey RJ, Gracious BL *et al*. (2007a). Methylphenidate in the treatment of children and adolescents with bipolar disorder and attention-deficit/hyperactivity disorder. *J Am Acad Child Adolesc Psychiatry* **46**: 1445–1453.

Findling RL, McNamara NK, Stansbrey RJ, Maxhimer R, Periclou A, Mann A *et al*. (2007b). A pilot evaluation of the safety, tolerability, pharmacokinetics, and effectiveness of memantine in pediatric patients with attention-deficit/hyperactivity disorder combined type. *J Child Adolesc Psychopharmacol* **17**: 19–33.

Gilbert DL, Ridel KR, Sallee FR, Zahng J, Lipps TD, Wassermann EM (2006). Comparison of the inhibitory and excitatory effects of ADHD medications methylphenidate and atomoxetine on motor cortex. *Neuropsychopharmacology* **31**: 442–449.

Goslin K, Banker G (1989). Experimental observations on the development of polarity by hippocampal neurons in culture. *J Cell Biol* **108**: 1507–1516.

Hamill OP, Marty A, Neher E, Sakmann B, Sigworth FJ (1981). Improved patch-clamp techniques for high-resolution current recording from cells and cell-free membrane patches. *Pflugers Arch* **391**: 85–100.

Jensen V, Rinholm JE, Johansen TJ, Medin T, Storm-Mathisen J, Sagvolden T *et al*. (2009). N-methyl-d-aspartate receptor subunit dysfunction at hippocampal glutamatergic synapses in an animal model of attention-deficit/hyperactivity disorder. *Neuroscience* **158**: 353–364.

Kielbasa W, Kalvass JC, Stratford R (2009). Microdialysis evaluation of atomoxetine brain penetration and central nervous system pharmacokinetics in rats. *Drug Metab Dispos* **37**: 137–142.

Kutsuwada T, Kashiwabuchi N, Mori H, Sakimura K, Kushiya E, Araki K *et al*. (1992). Molecular diversity of the NMDA receptor channel. *Nature* **358**: 36–41.

Lou HC (1996). Etiology and pathogenesis of attention-deficit hyperactivity disorder (ADHD): significance of prematurity and perinatal hypoxic-haemodynamic encephalopathy. *Acta Paediatr* **85**: 1266–1271.

Lulé D, Ludolph AC, Ludolph AG (2008). Neurodevelopmental and neurodegenerative diseases – Is there a pathophysiological link? Attention-deficit/hyperactivity disorder and amyotrophic lateral sclerosis as examples. *Med Hypotheses* **70**: 1133–1138.

Michelson D, Read HA, Ruff DD, Witcher J, Zhang S, McCracken J (2007). CYP2D6 and clinical response to atomoxetine in children and adolescents with ADHD. *J Am Acad Child Adolesc Psychiatry* **46**: 242–251.

Molina BS, Hinshaw SP, Swanson JM, Arnold LE, Vitiello B, Jensen PS *et al*. ; the MTA Cooperative Group (2009). The MTA at 8 years: prospective follow-up of children treated for combined type ADHD in a multisite study. *J Am Acad Child Adolesc Psychiatry* **48**: 484–500.

Monyer H, Burnashev N, Laurie DJ, Sakmann B, Seeburg PH (1994). Developmental and regional expression in the rat brain and functional properties of four NMDA receptors. *Neuron* **12**: 529–540.

Moore CM, Biederman J, Wozniak J, Mick E, Aleardi M, Wardrop M *et al*. (2006). Differences in brain chemistry in children and adolescents with attention deficit hyperactivity disorder with and without comorbid bipolar disorder: a proton magnetic resonance spectroscopy study. *Am J Psychiatry* **163**: 316–318.

Moriyoshi K, Masu M, Ishii T, Shigemoto R, Mizuno N, Nakanishi S (1991). Molecular cloning und characterization of the rat NMDA receptor. *Nature* **354**: 31–37.

Pittenger C, Duman RS (2008). Stress, depression, and neuroplasticity: a convergence of mechanisms. *Neuropsychopharmacology* **33**: 88–109.

Polanczyk G, de Lima MS, Horta BL, Biederman J, Rohde LA (2007). The worldwide prevalence of ADHD: a systematic review and metaregression analysis. *Am J Psychiatry* **164**: 942–948.

Sauer JM, Ring BJ, Witcher JW (2005). Clinical pharmacokinetics of atomoxetine. *Clin Pharmacokinet* **44**: 571–590.

Scherer D, Hassel D, Bloehs R, Zitron E, von Löwenstern K, Seyler C *et al*. (2009). Selective noradrenaline reuptake inhibitor atomoxetine directly blocks hERG currents. *Br J Pharmacol* **156**: 226–236.

Seneca N, Gulyás B, Varrone A, Schou M, Airaksinen A, Tauscher J *et al*. (2006). Atomoxetine occupies the norepinephrine transporter in a dose-dependent fashion: a PET study in nonhuman primate brain using (S,S)-[18F]FMeNER-D2. *Psychopharmacology* **188**: 119–127.

Sernagor E, Kuhn D, Vyklicky L, Mayer ML (1989). Open channel block of NMDA receptor responses evoked by tricyclic antidepressants. *Neuron* **2**: 1221–1227.

Sobolevsky AI, Yelshansky MV (2000). The trapping block of NMDA receptor channels in acutely isolated rat hippocampal neurons. *J Physiol* **526**: 493–506.

Swanson CJ, Perry KW, Koch-Krueger S, Katner J, Svensson KA, Bymaster FP (2006). Effect of the attention deficit/hyperactivity disorder drug atomoxetine on extracellular concentrations of norepinephrine and dopamine in several brain regions of the rat. *Neuropharmacology* **50**: 755–760.

Szasz BK, Mike A, Karoly R, Gerevich Z, Illes P, Vizi ES *et al*. (2007). Direct inhibitory effect of fluoxetine on n-methyl-d-aspartate receptors in the central nervous system. *Biol Psychiatry* **62**: 1303–1309.

Szobot CM, Ketzer C, Parente MA, Biederman J, Rohde LA (2004). The acute effect of methylphenidate in Brazilian male children and adolescents with ADHD: a randomized clinical trial. *J Atten Disord* **8**: 37–43.

Witcher JW, Long A, Smith B, Sauer JM, Heilgenstein J, Wilens T *et al*. (2003). Atomoxetine pharmacokinetics in children and adolescents with attention dieficit hyperactivity disorder. *J Child Adolesc Psychopharmacol* **13**: 53–63.

Woodhull AM (1973). Ionic blockage of sodium channels in nerve. *J Gen Physiol* **61**: 687–708.

Wrighton DC, Baker EJ, Chen PE, Wyllie DJA (2008). Mg^{2+} and memantine block of rat recombinant NMDA receptors containing chimeric NR2A/2D subunits expressed in Xenopus laevis oocytes. *J Physiol* **586**: 211–225.